

# Subtle Structural Aspects of Propylene-Based Copolymers as Revealed by Raman Spectroscopy

Mariela Desimone, Carla D. Mana, C. Javier Perez, José M. Carella, J. Pablo Tomba\*

*Institute of Materials Science and Technology (INTEMA), National Research Council (CONICET), University of Mar del Plata, Juan B. Justo 4302, 7600 Mar del Plata, Argentina*

Raman spectroscopy is used to elucidate fine details of the rather complex microstructure of ethylene-propylene copolymers (EPCs). This paper is focused on a series of commercial EPCs (Versify by Dow) with well-characterized ethylene content. Particular emphasis is given on the analysis of crystal type and content and their relation with EPC chain microstructure. Information provided by Raman is compared with that obtained by differential scanning calorimetry (DSC), a well-established technique widely used in the polymer field. Temperature-resolved Raman experiments are also carried out to interpret more precisely the complex melting patterns observed in the DSC traces. These experiments reveal precisely the crystal chemical composition and melting temperature ranges of EPC samples, key features to design processing conditions that guarantee optimum lifetime and recyclability of overmolded parts.

Index Headings: **Raman spectroscopy; Ethylene-propylene copolymers; EPCs; Crystallinity; Microstructure.**

## INTRODUCTION

Copolymerization is an effective way to create new families of polypropylene (PP) based polymers with improved elastic recovery and impact behavior, particularly useful for applications at sub-ambient temperatures. For instance, copolymerization with ethylene gives rise to ethylene-propylene copolymers (EPCs) with reduced crystallinity and lower glass transition temperature, the base of a vast family of products that combine in different proportions thermoplastic and elastomeric behaviors.<sup>1</sup>

In EPCs with relatively high propylene content, the insertion of ethylene units into the polymer backbone disturbs chain regularity, thus hindering the crystallization of propylene segments. Modern metallocene-based catalysis allows precise control of the distribution of ethylene units either in nearly random fashion (i.e., Vistamaxx from Exxon)<sup>2</sup> or in more blocky structures (i.e., Versify from Dow).<sup>3</sup> These different chain microstructures are expected to influence lamellar thickness and overall crystallinity in different ways. For instance, the existence of long sequences of ethylene units anticipates the presence of crystals of this type in addition to those formed by propylene units. The latest generations of catalysts also allow a high degree of control over the incorporation of regio- and stereo-defects, structural irregularities that disrupt the main chain regularity in a way similar to the insertion of co-

monomer units, adding another degree of freedom in the control of microstructure.

The resulting crystalline structure of EPCs is an interplay of these factors and can be actually very complex. Overall crystallinity, type of crystals, and melting temperature ranges are key features, as they lastly determine final properties, processing conditions, and prospective applications of the product. In terms of applications, we highlight those that involve the adhesion of EPC soft components over other more rigid polyolefinic cores, as found in automotive interiors, medical devices, telephone keypads, toothbrushes, shaving hardware, household appliances, or hand tools: in these systems, characterization of structural EPC features is important to develop understanding of the adhesion mechanisms in order to design processing conditions that guarantee optimum lifetime and recyclability of the fabricated parts.<sup>4,5</sup>

We show here how Raman spectroscopy can be helpful to elucidate fine details of the rather complex microstructure of EPC. We focus on a series of commercial EPCs (Versify by Dow) with well-characterized ethylene content. The analysis of crystal type and content and their relation with EPC chain microstructure are particularly emphasized. We compare the information provided by Raman spectroscopy with that obtained by differential scanning calorimetry (DSC), a technique widely used in the polymer field to characterize crystal melting. Temperature-resolved Raman experiments were also carried out to interpret more precisely the complex melting patterns observed in the DSC traces. While the assignment of crystalline structure and chemical composition by DSC can solely be made on the basis of melting temperature ranges, Raman has the potential of unambiguously determining the chemical identity of the just melted crystals.

## EXPERIMENTAL

We used three commercial EPC samples, Versify grades 3000, 3300, and 3401 (Dow), whose main characteristics are summarized in Table I. The low-density polyethylene (PE) was a 203M grade from Dow. The polypropylene (PP) was provided by Cuyolen as grade 1100N. Samples, provided in pellet form, were compression molded in a hydraulic press for 10 min at 120–170 °C, depending on the polymer, under a pressure of 5 MPa. Afterwards, the specimens were cooled to room temperature by water recirculation while keeping the sample between the press plates. Final sample thicknesses were in the range 100–120 μm. Specimens for DSC and Raman test were directly taken from them.

21 Received 13 January 2015; accepted 16 June 2015.

\* Author to whom correspondence should be sent. E-mail: jptomba@fi.mdp.edu.ar.  
DOI: 10.1366/15-07871

**TABLE I. Samples used in this paper.**

Grade	Sample ID	Density <sup>a</sup> (g/cm <sup>3</sup> )	Crystallinity <sup>a</sup> (wt %)	Ethylene <sup>b</sup> (wt %/mol %)
3000	V30	0.888	44	3.7/5.4
3300	V33	0.866	11–17	13/18
3401	V34	0.863	14	25/33

<sup>a</sup> Data taken from Dow brochures.

<sup>b</sup> Measured by <sup>13</sup>C NMR.

Ethylene composition of EPC was determined from analysis of triads by <sup>13</sup>C nuclear magnetic resonance (NMR) in a Varian Innova 300 spectrometer at 75 MHz. Differential scanning calorimetry was performed in a Perkin Elmer Pyris 1. The DSC results correspond to the first heating step, carried out at rates of 10 °C/min, under N<sub>2</sub> atmosphere. Raman spectra were acquired in a Renishaw in-Via Reflex system with a 785 nm diode (300 mW), using a grating of 1200 grooves/mm. The incident laser power was reduced at 10% using internal filters. Temperature-resolved Raman spectra were taken in a Linkam cell THM-600 under N<sub>2</sub> atmosphere. A 50× (0.5 numerical aperture, or NA) long working distance (8 mm) Leica metallurgical objective was used in the excitation and collection paths. The samples were heated at a rate of 10 °C/min, up to reach the pre-established temperature, and held for 60 s to allow Raman data collection. Spectra were typically acquired in 4 s with four accumulations.

## RESULTS AND DISCUSSION

**Thermal Analysis and Melting Behavior.** As seen from Table I, the EPC samples have different ethylene content, in the 3–25 wt % range (5–33 mol %); that is, they are mostly composed of propylene. The overall crystal contents for all the samples are below the values reported for neat isotactic-PP, typically in the 50–60% range. Both density and crystallinity values of EPC decrease with the increase in ethylene content. Note that despite a large difference in ethylene content between V33 and V34 grades, their crystallinity values are comparable.

Differential scanning calorimetry heating traces for the EPC samples are shown in Fig. 1 along with that of neat isotactic-PP (twofold reduced), included for comparison. Ethylene-propylene copolymer thermograms show a decrease in melting enthalpy (overall peak area) compared to the 100 J/g observed in neat PP: 70 J/g (V30), 35 J/g (V33), and 25 J/g (V34). This decrease is most likely connected with the drop in EPC crystallinity, and it is basically in line with the results shown in Table I. The DSC trace of PP shows a narrow melting peak with a maximum at 163 °C. Differently, EPC samples show broad endotherms with melting peaks much below 163 °C. This indicates a reduction in the length of crystallizable sequences that translate to a decrease in lamellar thickness. The effect can be ascribed to the disruption in chain regularity that causes the formation of thinner crystals. The disruption can be caused either by the incorporation of ethylene units or by the presence of stereo- or regio-defects, as both factors can alter the

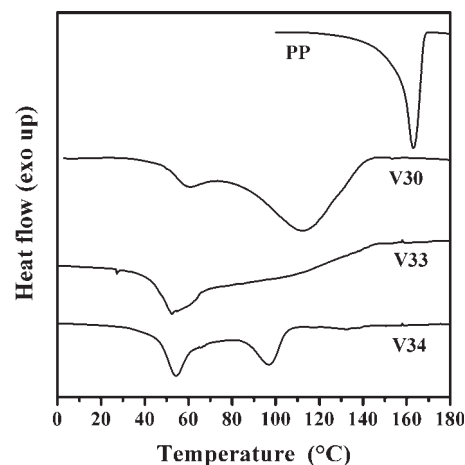


FIG. 1. Differential scanning calorimetry thermograms (heating step) of EPC and neat PP. The PP trace has been twofold reduced.

helix regularity along small chains sectors. The existence of multiple and well-defined melting peaks is observed in all EPC samples, in contrast with the single melting endotherm observed in neat PP. For instance, the V30 sample shows a broad peak with a maximum at 110 °C along with a minor second one centered at about 60 °C. The peak at higher temperature ends above 140 °C, consistent with an assignment to PP crystals. The lower temperature peak is in the range of melting temperatures usually associated with very thin PE crystals, as found for instance in some commercial ethylene-octene and ethylene-butene copolymers. However, the relatively low ethylene content of this sample (5.4 mol %), precludes this possibility. Thus, we might interpret the two melting peaks as representing two populations of PP crystals with different average thickness, assuming that the regular melting temperature-crystalline thickness relationships hold. The same view could explain the thermogram of V33, with predominance in this sample of PP crystals with lower melting temperatures.

The DSC trace of the V34 sample also shows two well-defined melting peaks centered at 52 and 97 °C, with a third, actually minor, at about 130 °C. As this sample has a relatively high ethylene content (33 mol %), one may wonder whether these melting peaks represent either crystals with different thickness of the same polymer, PP, as we have already tentatively assigned in V30 and V33, or crystals of a different nature, for instance, PP and PE. For the latter case, a reasonable assignment could be that the melting peak at 52 °C corresponds to PE crystals, whereas the other two at higher temperatures represent the melting of PP crystals. At this point, it is clear that DSC data are not conclusive and that we need more experimental evidence to confirm the nature of the crystalline phase.

**Structural Ethylene-Propylene Copolymer (EPC) Features from Raman Spectra.** Raman spectra at room temperature, that is, all the samples in the semi-crystalline state, are shown in Fig. 2 for the fingerprint region (700–1600 cm<sup>-1</sup>). In PP homopolymer, the region 750–880 cm<sup>-1</sup> is very useful to characterize crystal content.<sup>6</sup> The band at 810 cm<sup>-1</sup> has been ascribed to

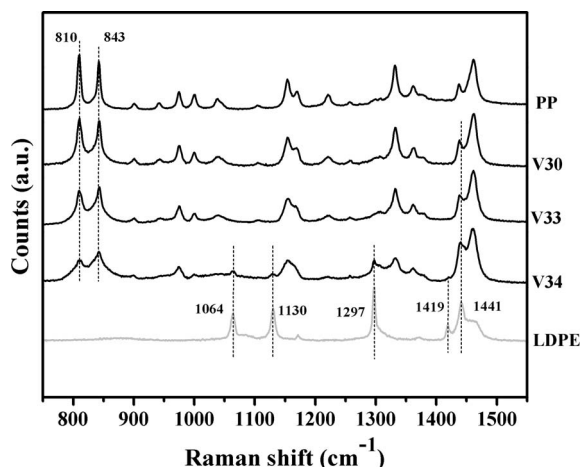


FIG. 2. Raman spectra of EPC, PP, and PE in the fingerprint region at 25 °C.

vibrational modes (rocking) of  $-\text{CH}_2-$  units in regular helical conformations, a clear signature of the presence of PP crystals. Bands at 843, 830, and 854  $\text{cm}^{-1}$  have been ascribed to the same vibrational mode, but for PP chains in disordered environments, as found in the amorphous part of a semi-crystalline polymer or in a melt.<sup>6,7</sup> In the spectrum of PP, the band at 830  $\text{cm}^{-1}$  appears as a small shoulder of the band at 843  $\text{cm}^{-1}$  that becomes more prominent with the increase in amorphous content. Eventually, bands at 830 and 843  $\text{cm}^{-1}$  merge into a single one when the sample is in the melt state, see results in the next section. The contribution of the band at 854  $\text{cm}^{-1}$  is in most of cases certainly minor, so in a first approach, we can simply trace PP crystallinity by the intensity ratio of the bands at 810 and 843  $\text{cm}^{-1}$  ( $I_{810}/I_{843}$ ). For neat PP, this ratio, as simply measured from peak heights, is about 1.25. However, the full set of bands and a rigorous curve fitting procedure should be accounted for quantitative calculations of crystallinity.<sup>7</sup>

On the other hand, ethylene signatures in EPC grades are expected to show up in two ways: (i) fundamental frequencies of  $-\text{CH}_2-$  units in disordered environments at 1080  $\text{cm}^{-1}$  (stretching), 1303  $\text{cm}^{-1}$  (twisting), and 1440  $\text{cm}^{-1}$  (bending), as observed in melted PE,<sup>8</sup> (ii) correlation splitting of these bands in the PE crystal lattice, as reflected by peaks at 1064 and 1130  $\text{cm}^{-1}$ , 1297  $\text{cm}^{-1}$ , and 1419 and 1441  $\text{cm}^{-1}$ , see the LDPE spectrum at 25 °C in Fig. 2.

In this framework, the Raman spectrum of V30 shows remarkable similarity to that of neat PP with basically the same band pattern. The ratio  $I_{810}/I_{843}$  is smaller (1.05) compared with that of neat PP (1.25), revealing an increase in amorphous content. No obvious features of the presence of ethylene units are seen, which is in some way expected due to the low ethylene content of this sample. The V33 sample continues this trend, showing even lower PP crystallinity ( $I_{810}/I_{843} = 0.87$ ). The spectrum of V33 shows subtle contributions of characteristic vibrational modes of ethylene units. For instance, the spectral profile in the 1400–1500  $\text{cm}^{-1}$  region is slightly different to that of PP, which can be explained by an increasing contribution of the peak at 1440  $\text{cm}^{-1}$ , characteristic of PE chains in amorphous

environments. A closer look to the spectrum of V30 in this region also shows that feature. On the other hand, as no clues of PE crystallinity are seen in any of these samples, we conclude that ethylene units in these V30 and V33 grades are mostly located in the amorphous phase.

The spectrum of the V34 sample is rather different to that of V30 or V33 with some remarkable band patterns. The intensity of the 810  $\text{cm}^{-1}$  band has noticeably decreased with respect to the 843  $\text{cm}^{-1}$  band ( $I_{810}/I_{843} = 0.64$ ). Prominent shoulders are now observed at both sides of the 843  $\text{cm}^{-1}$  peak, indicating a decrease in PP crystals content compared with the other EPCs. Remarkably, five small but discernible peaks at 1063, 1130, 1297, 1419, and 1440  $\text{cm}^{-1}$  are observed, revealing the unequivocal presence of PE crystal structures.<sup>8</sup>

The conclusion from Raman data is that V30 and V33 are essentially PP-based grades with ethylene units randomly distributed along the PP backbone. Ethylene units act, in this case, as points of disruption that decrease the length of crystallizable PP blocks, thus reducing crystal melting temperature and overall EPC crystallinity. The lack of ethylene triads observed by  $^{13}\text{C}$  NMR analysis (not shown) is consistent with this idea. This view does not certainly apply to V34. The fact that the Raman spectrum shows signatures of both PE and PP units in the crystalline phase leads us to think that the V34 sample has a blocky structure with ethylene and propylene units grouped separately in rather long sequences that allow the formation of separate types of crystals.  $^{13}\text{C}$  NMR analysis confirmed this blocky character as revealed by the large increase in the proportion of ethylene triads (12.6 wt %) compared with the other samples ( $\sim 0$  wt %). This blocky character is not surprising, as it has been reported as a signature of this new family of EPC.<sup>9</sup> They are referred to as showing a structure of block copolymers with gradual transitions in properties between blocks (tapered copolymers). A tapered monomer distribution may explain the two chemically different crystallizable blocks observed in V34. A control on the length of isotactic blocks may also well explain the two populations of PP crystals with different lamellar thickness observed in V30 and V33, an indication of isotactic PP sequences with different average lengths.

**Temperature-Resolved Raman Measurements.** We now address the point of how the above-described structural features, particularly the presence of mixed crystal structures in some of the EPC samples, correlates with the multiple melting peaks observed in the DSC data. To further investigate this issue, we carried out acquisitions of Raman spectra as a function of temperature. Figure 3a shows a series of Raman spectra for the PP sample, from room temperature to total melting. The peaks at 810 and 843  $\text{cm}^{-1}$  remained essentially invariant up to 140 °C, indicating that substantial melting has not occurred in this temperature range. The spectrum at 160 °C shows dramatic changes typical of melting. In the 800–900  $\text{cm}^{-1}$  region, the band at 810  $\text{cm}^{-1}$  (PP chains in the crystal lattice) has almost entirely disappeared, whereas the spectrum appears dominated by the 843  $\text{cm}^{-1}$  band (unoriented PP chains),

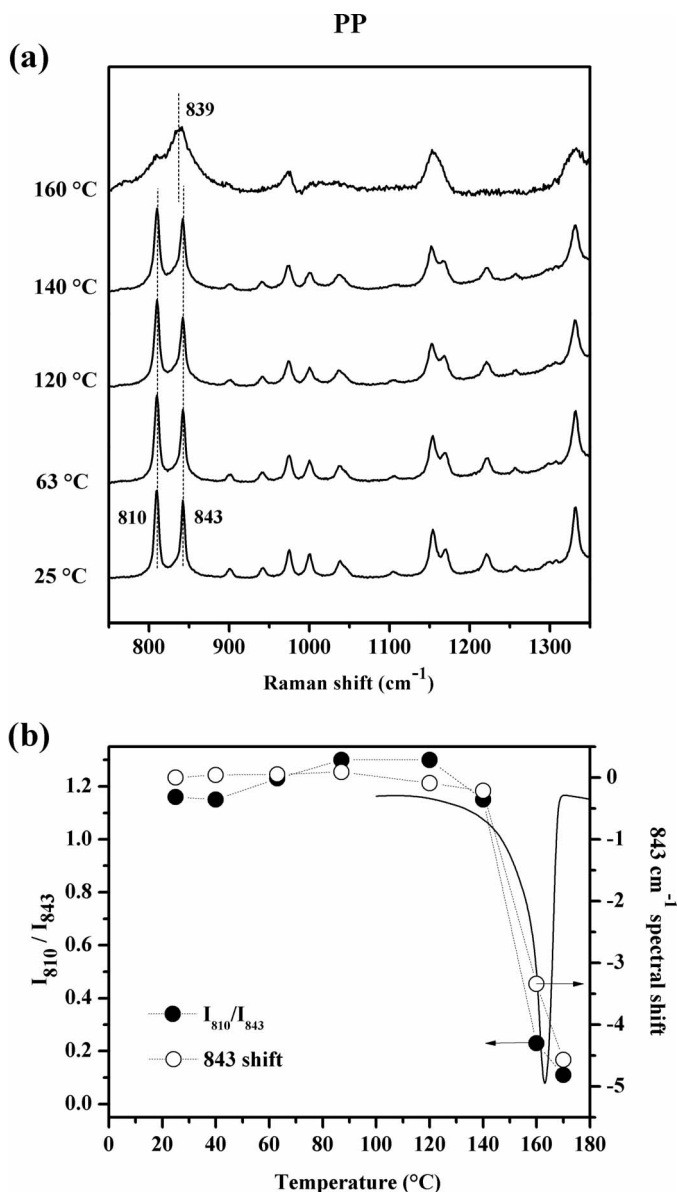


FIG. 3. (a) Raman spectra as a function of temperature for PP. (b) Evolution of band parameters as a function of temperature. The DSC trace is also included (solid line).

now low-shifted at about  $839\text{ cm}^{-1}$ . This spectral shifting is produced by the increasing contribution of the  $830\text{ cm}^{-1}$  band, ascribed to PP chains in disordered environments. This band, present as a small shoulder in the low temperature spectra, emerges superposed to  $843\text{ cm}^{-1}$  at higher temperatures with the eventual increase in PP amorphous content.

Both spectral features, either the change in  $I_{810}/I_{843}$  ratio or the degree of low-shifting of  $843\text{ cm}^{-1}$ , can be used to monitor changes in the PP crystal structure. Figure 3b shows the evolution of  $I_{810}/I_{843}$  ratio (left-hand x-axis) and degree of  $843\text{ cm}^{-1}$  low-shifting (right-hand x-axis) as a function of acquisition temperature. We have superposed the corresponding DSC trace in continuous line, for comparison. Remarkably, both band parameters show an abrupt change at the melting temperature of PP. The  $I_{810}/I_{843}$  ratio drops from values close to 1.2 at  $140\text{ }^{\circ}\text{C}$  to values below 0.2 at  $160\text{ }^{\circ}\text{C}$ . On the other hand, spectral

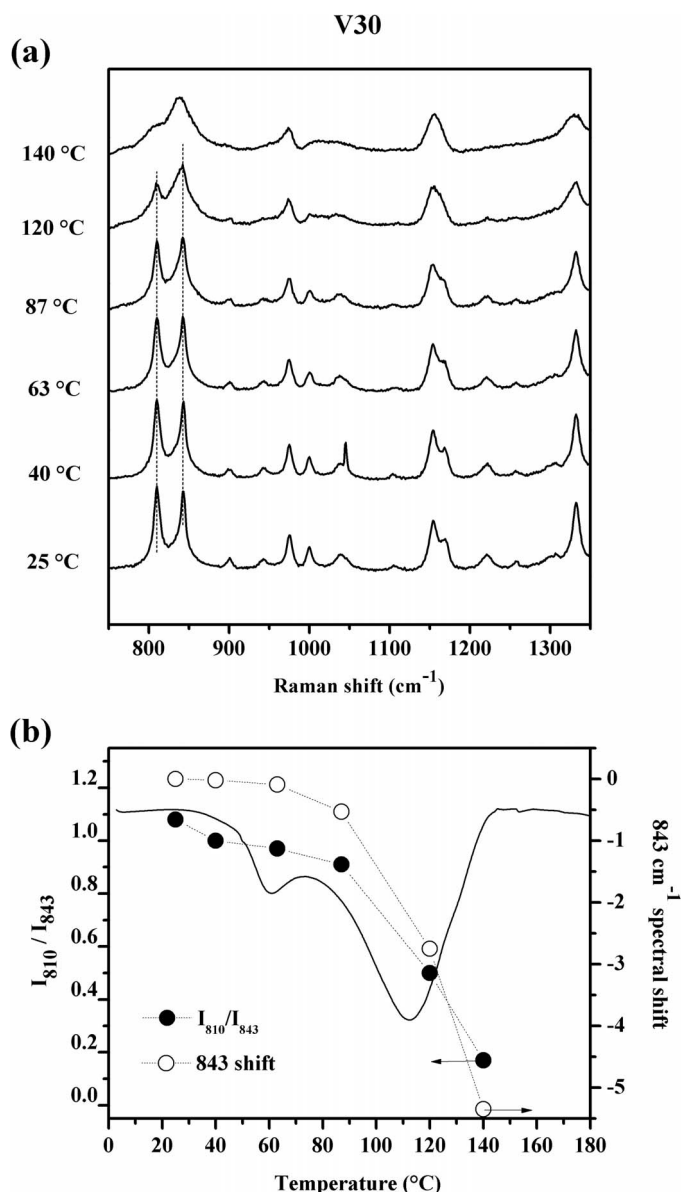


FIG. 4. (a) Raman spectra as a function of temperature for V30. (b) Evolution of band parameters as a function of temperature. The DSC trace is also included (solid line).

shifts of the  $843\text{ cm}^{-1}$  peak are almost negligible up to  $140\text{ }^{\circ}\text{C}$  but suddenly increase at about  $3.5\text{ cm}^{-1}$  units at  $160\text{ }^{\circ}\text{C}$ . Although the determination of the intensity ratios can be subjected to some error due to the very low intensity of  $810\text{ cm}^{-1}$  near melting, the detection of spectral shifts is rather straightforward as they can actually be very large upon melting. Overall, those spectral changes are in very good agreement with the melting temperature ranges of the single peak observed in the corresponding DSC trace, confirming that they are effectively sensing changes in the crystal structure of the propylene phase.

Figures 4a and 4b show Raman spectra and the evolution of band parameters for the V30 sample. The spectral evolution of V30 shows that the intensity of the  $810\text{ cm}^{-1}$  peak decreases with respect to  $843\text{ cm}^{-1}$ , first in a small amount (range  $25\text{--}87\text{ }^{\circ}\text{C}$ ) and then more markedly above  $87\text{ }^{\circ}\text{C}$ . The spectrum at  $140\text{ }^{\circ}\text{C}$  indicates

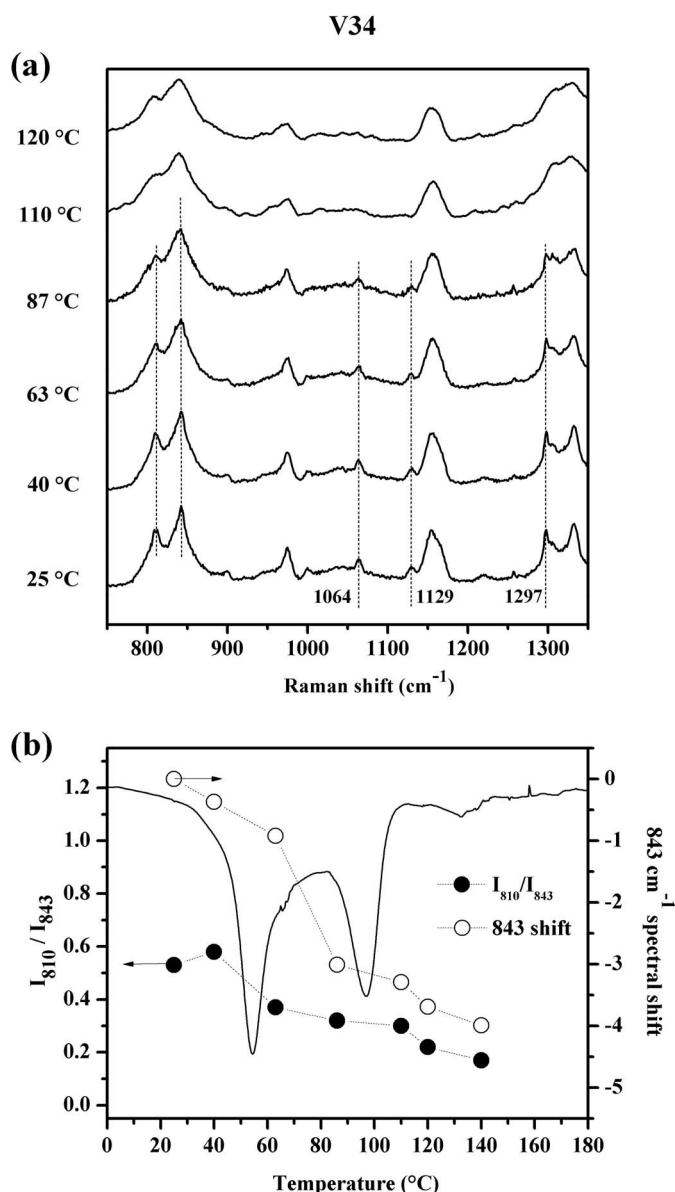


FIG. 5. (a) Raman spectra as a function of temperature for V34. (b) Evolution of band parameters as a function of temperature. The DSC trace is also included (solid line).

complete melting. This evolution is analyzed on a quantitative basis in Fig. 4b. The  $I_{810}/I_{843}$  ratio decreases from values close to 1.1 at room temperature to about 0.9 at 87 °C, followed by a large drop up to about 0.5 at 120 °C, indicative of almost complete melting. The shift in 843 cm⁻¹ also follows very well this trend; that is a minor but noticeable shift from 25–87 °C and a larger drop above 87 °C. Once again, the temperature ranges of each melting sequence of the PP crystalline phase observed by Raman are very well correlated with the two endotherms observed in the DSC data. The same good agreement between Raman and DSC data was found in V33 (not shown), with Raman profiles characterized by a major melting of PP crystals early (range 25–63 °C), until completion at 120 °C.

The evolution of the spectral pattern of the V34 sample, shown in Fig. 5, is anticipated to be interesting, considering the mixed crystalline structure found for this

sample. Raman spectra in Fig. 5a show a gradual reduction of the 810 cm⁻¹ peak (PP crystals) in the range 25–87 °C. Figure 5b shows the evolution of band parameters in comparison with the thermal profile of the DSC experiment. The  $I_{810}/I_{843}$  ratio shows a small but noticeable drop in the range 40–80 °C, reaching values of about 0.3, characteristic of almost total melting of PP crystals. The ratio does not show substantial changes above 80 °C, which indicates that most of the propylene crystals have melted below 80 °C. The trend is more clearly observed in the spectral shifts of 843 cm⁻¹ that reach values of about 3 cm⁻¹ at 80 °C. If we focus now our attention on PE crystals, Fig. 5a shows that the minor peaks attributed to PE crystals (1066, 1130, and 1297 cm⁻¹) remain essentially intact, even at temperatures as high as 87 °C. At 110 °C, Raman peaks of PE crystal units have disappeared, and at 120 °C, the sample is almost totally melted. Therefore, counter-intuitively, based solely on DSC melting temperature ranges, the low temperature peak in the DSC thermogram (52 °C) must be then associated with melting of PP crystals, whereas the peak at higher temperature (97 °C) can be assigned to PE crystals.

This remarkable observation illustrates the power of Raman spectroscopy in revealing complex and by no means evident structural details of EPC. It may appear at a first sight inconsistent with the fact that the intensity of Raman bands associated with PE crystal are actually much smaller compared with that of PP crystals, while the areas under melting peaks in DSC data look similar. At this point, we should consider that the melting enthalpy per gram of crystal is much higher in PE (about 280 J/g) than in PP (208–145 J/g, depending on the crystalline form).<sup>10–12</sup> The area of the peak assigned to PE in the thermograms is about 30% of the total melting area (25 J/g) so calculations of crystal content yield values of about 10 wt. % of PP, assuming an average value of 175 J/g,<sup>†</sup> and about 2–3% of PE, i.e., the mass of PP crystals is 3–4 times larger than that of PE crystals. On the basis that cross sections for Raman scattering of PE and PP are comparable, this ratio is in agreement with the observed spectral features.

## CONCLUSIONS

We have shown that Raman microscopy can be a very useful tool for the characterization of EPCs. The sensitivity of the Raman profile to specific vibrational modes of propylene and ethylene units in different environments provides a rich spectral picture that reflects several structural features of these materials. The technique was used to discriminate a series of commercial EPC samples with different ethylene content on the base of crystal type and content. From this information, details on copolymer architecture could be inferred. The evolution with temperature of band parameters associated to vibrations of PP chains in the crystal lattice was used to identify melting ranges of the different crystal populations. These results correlate

<sup>†</sup> Versify grades have substantial amounts of  $\gamma$  PP crystalline phase, as found in our X-ray diffraction patterns (not shown), see also Chum et al.,<sup>12</sup> so an average value of 175 J/g for PP crystals appears as a reasonable choice.

very well with the multiple endotherms observed in the DSC thermogram, but they provide a higher level of description, as Raman is able to identify the chemical nature of the crystals. For instance, it was found that samples with 33 mol % of ethylene are composed of an unusual mixed crystalline structure of high/low melting temperature ethylene/propylene crystals, details that are not evident in the DSC traces.

The level of information obtained, typically not provided by manufacturers, is very valuable in the context of problems of adhesion of EPCs onto other rigid polyolefinic substrates, where a detailed knowledge of temperature melting ranges and crystal nature becomes crucial to control chain penetration or co-crystallization and, in turn, the optimum degree of adhesion between parts.<sup>4,5,13</sup> Other useful information, such as EPC chemical composition, the identification of crystalline isomorphs, or the capabilities for spatially resolved measurements, complete the range of potential applications. In a broader perspective, Raman microscopy provides a rather complete characterization platform for EPC products in a single technique.

#### ACKNOWLEDGMENTS

This work was supported by National Agency for the Promotion of Science and Technology (PICT10-284, PICT14-1919) and National University of Mar del Plata (ING358/12), Argentina.

1. The Dow Chemical Company. "Engage Polyolefin Elastomers | Dow Elastomers". 995–2015. <http://www.dow.com/elastomers/products/engage.htm> [accessed Sep 2 2015].
2. S. Toki, I. Sics, C. Burger, D. Fang, L. Liu, B.S. Hsiao, S. Datta, A.H. Tsou. "Structure Evolution During Cyclic Deformation of an Elastic

- Propylene-Based Ethylene-Propylene Copolymer". *Macromolecules*. 2006. 39(10): 3588-3597.
3. P.S. Chum, K.W. Swogger. "Olefin Polymer Technologies—History and Recent Progress at the Dow Chemical Company". *Prog. Polym. Sci.* 2008. 33(8): 797-819.
4. M. Dondero, J.M. Pastor, J.M. Carella, C.J. Perez. "Adhesion Control for Injection Overmolding of Polypropylene with Elastomeric Ethylene Copolymers". *Polym. Eng. Sci.* 2009. 49(10): 1886-1893.
5. Y. Lin, G.R. Marchand, A. Hiltner, E. Baer. "Adhesion of Olefin Block Copolymers to Polypropylene and High Density Polyethylene and Their Effectiveness as Compatibilizers in Blends". *Polym.* 2011. 52(8): 1635-1644.
6. S. Nielsen, D.N. Batchelder, R. Pyrz. "Estimation of Crystallinity of Isotactic Polypropylene Using Raman Spectroscopy". *Polym.* 2002. 43(9): 2671-2676.
7. C. Minogianni, K.G. Gatos, C. Galiotis. "Estimation of Crystallinity in Isotropic Isotactic Polypropylene with Raman Spectroscopy". *Appl. Spectrosc.* 2005. 59(9): 1141-1147.
8. G.R. Strobl, W. Hagedorn. "Raman Spectroscopic Method for Determining the Crystallinity of Polyethylene". *J. Polym. Sci. Pol. Phys.* 1978. 16(7): 1181-1193.
9. D. Sexton, P. Ansens, L. Hazlitt. "Plastic Innovation from Dow International Polyolefins". Versify technical papers. Houston, Texas: [www.dow.com](http://www.dow.com). 2004.
10. J. Varga. "Supermolecular Structure of Isotactic Polypropylene". *J. Mater. Sci.* 1992. 27(10): 2557-2579.
11. K. Mezghani, P.J. Phillips. "The  $\gamma$ -Phase of High Molecular Weight Isotactic Polypropylene: III. The Equilibrium Melting Point and the Phase Diagram". *Polym.* 1998. 39(16): 3735-3744.
12. S. Chum, C.H. Stephens, B. Poon, P. Ansens, A. Hiltner, E. Baer. "Solid State Properties of New Propylene-Ethylene (p/e) Copolymers". Paper presented at: SPE ANTEC Conference, Nashville, TN. 2003. Pp. 1775-1779.
13. S. Nguyen, C.J. Perez, M. Desimone, J.M. Pastor, J.P. Tomba, J.M. Carella. "Adhesion Control for Injection Overmolding of Elastomeric Propylene Copolymers on Polypropylene. Effects of Block and Random Microstructures". *Int. J. Adhes. Adhes.* 2013. 46: 44-55.

22

**Queries for apls-69-12-16**

- 1. Author: This article has been edited for grammar, and journal style and usage. Please compare it with your original document and make corrections on these pages. Please limit your corrections to substantive changes that affect meaning. If no change is required in response to a question, please respond "OK as set." Copyeditor**
- 2. Author: Please verify information in Ref. 9. Copyeditor**